

CdS Nanocrystals in Chelate Polymer Microparticles: Polymer Size Dependence of The Optical Properties

Hiroshi Yao* and Noboru Kitamura

Department of Chemistry, Faculty of Science, Hokkaido University, Kita-ku, Sapporo 060

(Received November 10, 1995)

CdS nanocrystals were prepared in micrometer-sized chelate polymer particles by nucleation of Cd^{2+} ions with an aqueous Na_2S solution. Simulation of the absorption spectral band shapes of CdS under an effective mass approximation was conducted on the basis of the size distributions of the crystals in the polymer, which were estimated by the relevant transmission electron micrograph images. The optical properties and the size distributions of CdS were dependent on the diameter of the polymer particle, when the concentration of an added S^{2-} solution was sufficiently high for rapid nucleation. In the case of the reaction of Cd^{2+} with a diluted S^{2-} solution, contrarily, the formation of CdS was confined in the surface layer of the host polymer particle with layer-by-layer size distributions. Effects of the host polymer particle size and the concentration of the Na_2S solution on the size distributions and the optical properties of CdS are discussed in terms of the apparent rate of nucleation of Cd^{2+} to CdS.

There has been a significant increase in interest in nanometer-sized semiconductor crystals (nanocrystals) which belong to a state of matter in the transition region between molecules and bulk solids. A variety of studies on nanocrystals have been conducted so far in special reference to quantum size effects, nonlinear optical phenomena, and unusual fluorescence characteristics associated with surface structures.^{1–3)} Among these studies, preparations of size-controlled, monodispersed semiconductor nanocrystals are of primary importance for further progress in the field, and several methods such as hexametaphosphate stabilization,⁴⁾ reversed micelles,⁵⁾ size-selective precipitation stabilized with 3-mercapto-1,2-propanediol,⁶⁾ and surface passivation with trialkylphosphine chalcogenide⁷⁾ have been developed for production of CdS and CdSe nanocrystals. Dense dispersion of nanocrystals and understanding of the relevant dispersion characteristics in dielectric host media are also desired for fundamental physics and device applications.^{8,9)} However, since a single nanocrystal consists of only a small number of atoms (100—10000), an elucidation of the interactions between the crystal surface and the host matrices is absolutely necessary to understand the electronic properties of nanocrystals.¹⁰⁾

Solid matrices such as glasses and polymers act as dielectric host matrices and are considered to be useful for preventing particle flocculation. In particular, polymer matrices are very interesting¹¹⁾ since interactions between nanocrystal surfaces and functional molecular groups in polymers are expected to be controlled by the properties of the host polymers. Therefore, we have explored the preparation of CdS nanocrystals in micrometer-sized chelate polymer particles. The use of polymer particles having chelating ligands is very favorable for homogeneous and dense loading of Cd^{2+} ions in the host matrix via interactions between the ion and the ligand.¹²⁾ When CdS crystals grow in the polymer particle

by nucleation of Cd^{2+} with an appropriate S^{2-} source, the crystal size and distribution, morphological structures, and their electronic properties will be affected by the electrostatic interactions between the crystal surface and the ligands. According to a theoretical model of ion-exchange mechanisms in polymer resin beads, furthermore, the reaction of Cd^{2+} ions with a sulfur source is expected to be controlled through several factors such as the concentration of the sulfur source and the surface area of the polymer particle.¹³⁾ Although characterization of a single microparticle is in general difficult, we have already established a microspectroscopy technique, applicable to a single microparticle in solution, so that the optical properties of CdS nanocrystals can be studied for individual polymer particles.

In this article, we report the preparation and characterization of CdS nanocrystals embedded in chelate polymer particles. A particular emphasis of the report is the observation of a polymer size dependence of the optical properties of CdS nanocrystals. To elucidate this polymer size effect, we conducted simulation of the absorption spectra of CdS on the basis of a theoretical model by Roussignol et al. and size distributions of CdS in the host polymer.¹⁴⁾ Peculiar dispersion structures of CdS in polymer particles observed under certain preparation conditions and the factors governing the size and the distribution of CdS are described.

Experimental

Chemicals. Chelate polymer microparticles (Chelex 100: 200—400 mesh, Analytical Grade, Bio-Rad Laboratories) made of styrene-divinylbenzene copolymers having iminodiacetate groups were used as a host matrix to prepare CdS nanocrystals. The beads were soaked in distilled water and washed successively with methanol, aqueous HCl (2 M, $\text{M}=\text{mol dm}^{-3}$), aqueous NaOH solutions (2 M), and then thoroughly with water. After treating with etha-

nol, the beads were dried under vacuum. Cadmium acetate $\text{Cd}(\text{CH}_3\text{COO})_2 \cdot 2\text{H}_2\text{O}$ (GR grade, Kojima Chemicals) and sodium sulfide $\text{Na}_2\text{S} \cdot 9\text{H}_2\text{O}$ (GR grade, Wako Pure Chemicals) were used as received.

Sample Preparations. The chelate polymer (0.087 g, dried weight) was soaked in an aqueous $\text{Cd}(\text{CH}_3\text{COO})_2$ solution (0.1 M, 0.5 mL) for 10 min under supersonication, and stored for 2 d at room temperature. All the Cd^{2+} ions were confirmed to be incorporated into the polymer, as judged by the fact that the supernatant solution no longer reacted with S^{2-} ions to form CdS. The Cd^{2+} -incorporated chelate polymer was then washed with distilled water several times. Preparations of CdS nanocrystals in the polymer were performed by adding an aqueous Na_2S solution to the Cd^{2+} -polymer samples. Diffusion of S^{2-} ions into the polymer particles is expected to depend on the initial concentration of S^{2-} . Therefore, we prepared CdS-polymer samples by the following two methods employing different initial concentrations of the Na_2S solution.

Sample a: The Cd^{2+} -polymer beads described above were redispersed in 1 mL of water and 2.6 mL of an aqueous Na_2S solution (1.8×10^{-2} M) were added into the solution with vigorous stirring. The polymer particles immediately turned pale yellow due to CdS formation. After stirring for 30 min, the mixture was left standing for 1 d. The supernatant solution was removed and the particles collected by suction filtration were washed repeatedly with water and ethanol. The sample was then dried in vacuo.

Sample b: A dilute Na_2S solution was used to prepare CdS nanocrystals. In order to adjust the total amount of the S^{2-} ion to that in sample a, 50 mL of an aqueous Na_2S solution (9.2×10^{-4} M) were added to the Cd^{2+} -polymer particles (0.087 g, dried weight) dispersed in 10 mL of water. The solution was stirred for 2 h and then left standing for 1 d. After working up procedures analogous to those for sample a, the particles were dried under vacuum.

Measurements. Absorption spectra of CdS in single polymer particles were measured by a microspectroscopy system consisting of an optical microscope and a polychromator-multichannel photodetector set as reported previously.¹⁵⁾ A 150 W Xe lamp was used as a light source for absorption spectroscopy. In the case of the dried CdS-polymer samples, the incident Xe beam was scattered by the particle under the microscope, so that the sample was dispersed in water to reduce light scattering. The chelate polymers swelled in water approximately ca. 1.5 times and the diameter of the particles was determined for the solution samples. Chelex 100 did not show any absorption in the wavelength region above ca. 400 nm. For the calculation of absorbance, therefore, the incident light intensity (I_0) was determined by the light beam being passed near a sample particle, while the transmitted light intensity through a CdS-polymer particle (I) was measured by passing the beam at the center of the particle. For dye-doped Chelex 100 particles, we confirmed that these procedures afforded reproducible spectra with a spectral resolution and minimum absorbance of 2 nm and 0.05, respectively.¹⁶⁾ In the present study, the particles were as large as ca. 100 μm and the Brownian motion in water was almost indiscernible. Therefore, we performed absorption spectroscopy without laser trapping of the particles. Transmission electron microscopy (TEM) was conducted by a JEM2010 electron microscope (JEOL). The CdS-polymer particles were fixed in epoxy resin and the resin was thinly sliced for the TEM measurements.

Simulation of the Absorption Spectra. Simulation of the absorption spectra of sample a was performed based on a theoretical model reported by Roussignol et al.¹⁴⁾ Under an effective mass approximation, we assume that an electron-hole pair is confined in a sphere of radius R ($=d_{\text{CdS}}/2$, where d_{CdS} is the crystal diameter) with

an infinite potential barrier. In this model, the transition energies of a CdS nanocrystal (E_{n1}^{R}) are described as in Eq. 1.

$$E_{n1}^{\text{R}} = E_g + \hbar^2 \phi_{n1}^2 / (8\pi^2 m^* R^2) - 1.8e^2 / (\epsilon R) \quad (1)$$

where E_g is the band gap energy of bulk CdS (2.5 eV).¹⁷⁾ The second term represents the confined kinetic energy of a particle, where m^* is the effective reduced mass taken here to be approximately 0.2 m_0 ¹⁷⁾ as a mobile electron mass and ϕ_{n1} is the n -th root of the spherical Bessel function of 1-th order. In the present study, we consider the lowest three quantized transition energies of 1S–1S, 1P–1P, and 1D–1D which correspond to ϕ_{10} ($=3.14$), ϕ_{11} ($=4.49$), and ϕ_{12} ($=5.75$), respectively. The Coulomb interaction energy between an electron and a hole in a semiconductor with a dielectric constant of ϵ was taken as the third term of the right-handed side of Eq. 1.^{1,18)} Although the spin-orbit splitting interaction would be considered for any three transitions, this might lead to an overestimation of homogeneous broadening tails in the simulation. Therefore, only the transition from the 1S spin-orbit split-off band ($\Delta_{\text{SO}}=64$ meV¹⁹⁾) to the lowest 1S electron level was taken into account.²⁰⁾ The absorption coefficient $\alpha^{\text{R}}(\omega)$ at a given frequency (ω) is the sum of the contributions from the 1S–1S, 1S_{SO}–1S, 1P–1P, and 1D–1D transitions and each transition possesses a homogeneous line width of $1/T_2$ and an intensity caused by level degeneracies.¹⁴⁾ A crystal size distribution can be expressed as a log normal distribution function $f(R)$ with a standard deviation of σ , as confirmed by analyzing a TEM image of the samples (discussed later),

$$f(R) = \frac{1}{(2\pi)^{1/2} \sigma} \exp \left[-\frac{\ln^2(R/R_0)}{2\sigma^2} \right], \quad (2)$$

where R_0 is a center radius of the distribution. The absorption spectral shape ($\alpha(\omega)$) can be simulated by Eq. 3 by taking a proportional factor of k into account.

$$\alpha(\omega) = k \int \alpha^{\text{R}}(\omega) f(R) \cdot d\ln(R). \quad (3)$$

In actual simulation, the line shape parameter (T_2) was fixed to 10 fs²¹⁾ and the absorption spectrum was fitted by two parameters: σ and R_0 .

Results and Discussion

Optical Properties of CdS Nanocrystals in Chelate Polymer Particles. Figures 1a and 1b show the absorption spectra of CdS in individual polymer particles prepared from the concentrated (sample a) and dilute (sample b) aqueous Na_2S solutions, respectively. It is noteworthy that the S/N values of the spectra around 400–420 nm are worse compared with those in the longer wavelength region. This is because transmittance of the microscope objective decreases with shifting incident light (I_0) to the shorter wavelength, particularly, below 420 nm. However, the present microspectroscopy technique enabled reproducible measurements of the spectra for individual polymer microparticles (see the Experimental section), so that quantitative discussion could be made on the basis of the data in Fig. 1.

As clearly seen in Fig. 1, the absorption spectra of CdS were strongly dependent on the preparation method. The important results are as follows. Firstly, the onset wavelength, below which the absorbance increased sharply, was around 500 nm for sample a while that for sample b was shifted to a longer wavelength (520 nm). For CdS crystals, it is well-

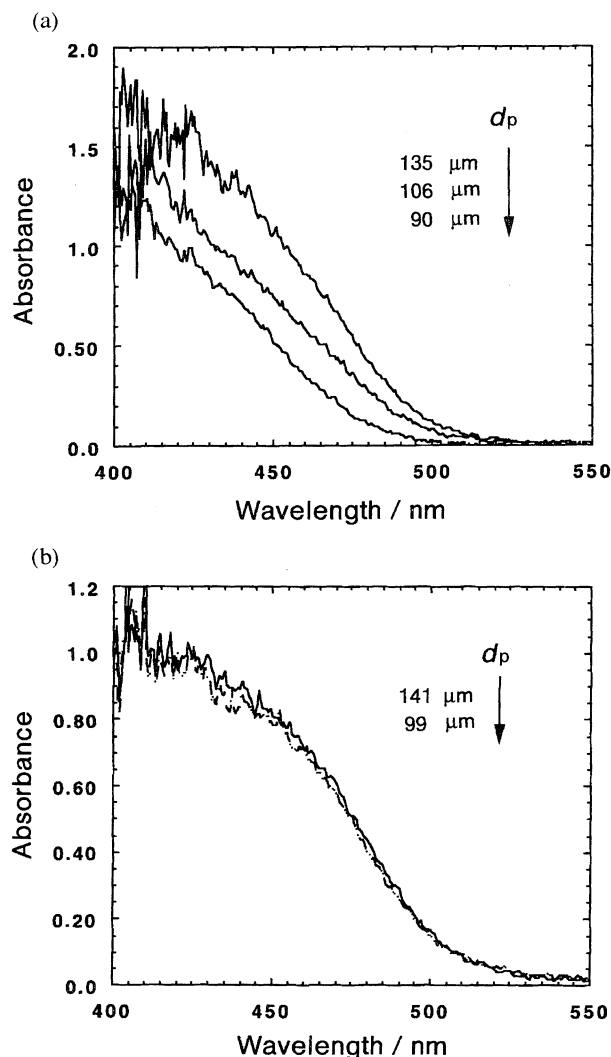


Fig. 1. Absorption spectra of CdS nanocrystals embedded in the chelate polymers. a) sample a from concentrated Na_2S solution, b) sample b from dilute Na_2S solution.

known that the onset wavelength shifts to a shorter one with decreasing crystal size. Actually, Weller and his co-workers have reported that the band gap energy, related to the onset wavelength of CdS, increases from 2.4 to 3.9 eV with decreasing average CdS diameter from 9.6 to 1.4 nm.⁶⁾ As judged from the spectra in Fig. 1 and those reported by Weller et al., CdS crystals with a diameter of several nanometers are expected to be produced in the chelate resin beads. Secondly, the onset wavelength strongly depended on the diameter of the host matrix (d_p) for sample a while that for sample b was almost constant irrespective of d_p (100–140 μm). Figure 1a clearly demonstrates that the onset wavelength shifts toward a shorter wavelength with decreasing d_p . Furthermore, the absorbance of CdS for sample b was almost independent of d_p , which was in marked contrast to the results for sample a. As a general feature of the present results, the CdS cluster size is controlled by the concentration of added Na_2S and the diameter of the host polymer bead.

Distributions of CdS Nanocrystals in Chelate Polymer

Particles. The absorbance of CdS with similar d_{CdS} embedded in the polymer should increase with an increase in d_p , if d_p is equal to the optical path length for absorption measurements. Therefore, the difference in the d_p dependence of the absorption spectra in Fig. 1 indicates those in distributions of CdS between samples a and b. In order to investigate distributions of CdS nanocrystals in the polymer particles, we performed transmission electron microscopy (TEM) measurements. Figure 2 shows the TEM images of both surface and center areas of the CdS-polymer samples a and b. For sample a, the TEM pictures in Figs. 2a and 2b demonstrate that small CdS nanocrystals (recognized as black spots) are dispersed densely and homogeneously in both the surface layer and the center area of the polymer particle. According to the results from the TEM observation, the size distribution of CdS is fairly narrow with a crystal diameter (d_{CdS}) of ca. 3 nm. The results agree with the d_p dependence of the absorption spectra. In Fig. 1a, actually, the increase in d_p from 90 to 135 μm (1.5 fold) results in an absorbance of ca. 1.5 at 420 nm, indicating that the diameter of the polymer particle corresponds to the optical path length. On the basis of both absorption and TEM experiments, we conclude that CdS nanocrystals are distributed homogeneously in the entire host matrix of sample a. The size distribution of CdS in sample a ($d_p=135 \mu\text{m}$) determined by the TEM image (Fig. 2a) is shown in Fig. 3. It is noteworthy that the size distribution can be well fitted by the log normal distribution function in Eq. 2 with parameters of $2R_0=2.7 \text{ nm}$ and $\sigma=0.37$. This is the important result for simulation of the absorption spectral shape of CdS, as described in the following section.

For sample b, on the other hand, interesting and peculiar dispersion textures were found in the TEM image as shown in Fig. 2c, in which the polymer particle boundary is indicated by the arrow in the photograph. Although it is not clear from Fig. 2c due to the low magnification ($\times 10000$) of the image, CdS crystals are precipitated homogeneously in the surface layer (ca. 5 μm in thickness) of the polymer particle. Actually, the image of this area at a higher magnification ($\times 300000$, Fig. 2d) proves no flocculation of CdS and the average diameter of the crystals has been shown to be ca. 3 nm. On going from the particle surface to the inner area, the size of the CdS crystals increases as can be recognized by the fact that the morphology changes from the upper left (surface) to the lower right (inner part) in Fig. 2c. The magnified TEM image of the area inner from the surface by ca. 5 μm shown in Fig. 2e indicates that CdS nanocrystals with a diameter of 5–7 nm flocculate each other to produce larger particles with a diameter of 20–30 nm. It is noteworthy that no CdS crystals can be observed at the central part of the polymer bead, so that sample b possesses layer-by-layer distributions of CdS. Therefore, the determination of a size distribution function was very difficult for sample b. The formation of CdS nanocrystals in the surface layers of the polymer particle coincides very well with the absence of a d_p dependence of the absorption spectrum (Fig. 1b). The optical properties of CdS nanocrystals are governed by the sample preparation method (i.e., concentration of the added

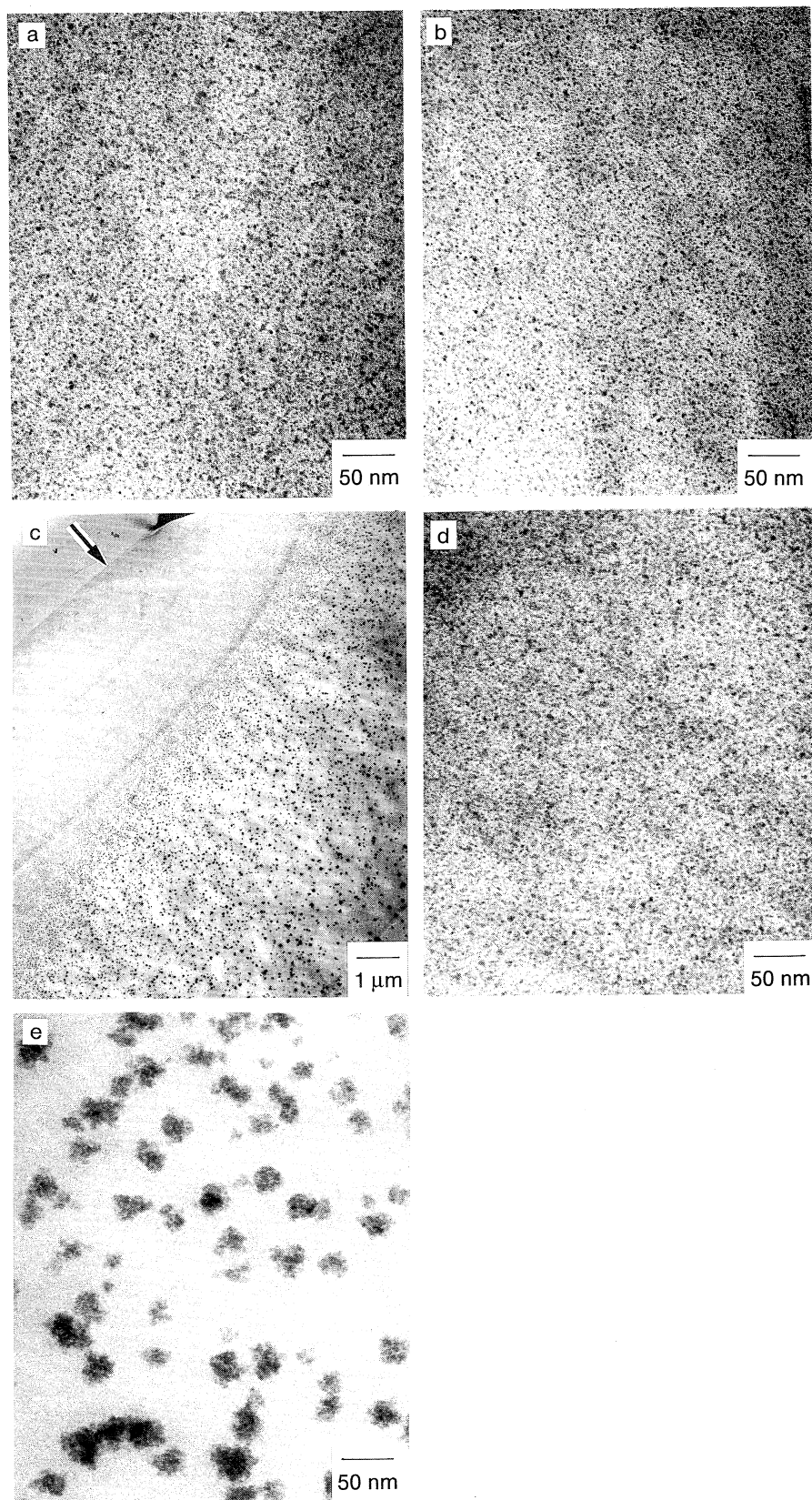


Fig. 2. TEM images of the CdS-polymer particles. a) and b) show the surface and center images of the particle (sample a, $\times 300000$), respectively. c) and d) represent TEM images of the surface areas of the particle (sample b) with the magnification of 10000 and 300000, respectively. e) is the image of the particle (sample b) ca. 5 μm inner from the surface ($\times 300000$). The arrow indicated in Fig. 2c represents the polymer particle boundary.

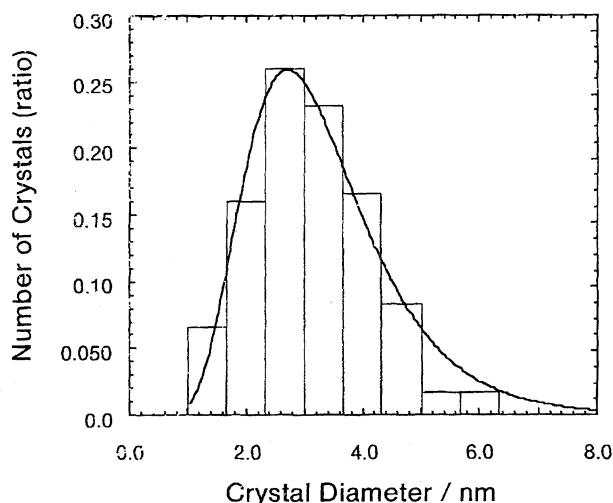


Fig. 3. Observed (histogram) crystal size distribution of sample a ($d_p = 135 \mu\text{m}$) and the fitted log normal distribution function (solid curve). The histogram were obtained from the TEM images in Fig. 2a.

Na_2S solution) through the changes in the distributions of the crystals in the host polymer particles (discussed later).

Simulation of the CdS Distribution in Polymer Particles. In order to reveal the optical properties and the size distribution of the CdS nanocrystals in the polymer, detailed analyses of the samples by X-ray diffraction, small-angle X-ray scattering, and so forth are preferable. However, such analyses are very difficult for the present samples, since the properties of CdS nanocrystals are dependent on d_p (sample a). Also, analyses of single polymer particles are in general very difficult except for those by absorption and emission spectroscopy. Since one of the principal aims of this research is to elucidate the origin of the polymer size dependence of d_{CdS} and the size distribution, we conducted simulation of the absorption spectral band shape of CdS for sample a.

The d_{CdS} distributions of sample a shown in Fig. 3 can be fitted by a log normal function as described in the preceding section. Actually the observed spectrum of the CdS-polymer particle with $d_p = 135 \mu\text{m}$ was reproduced fairly well by using a function with $2R_0 = 2.7 \text{ nm}$ and $\sigma = 0.37$, except for the absorption tail towards 550 nm . The results indicate that the crystal size distributions can be estimated from the absorption spectra. Therefore, we also conducted simulation of the absorption spectra of the CdS-polymer particle with $d_p = 106$ and $90 \mu\text{m}$ and the results are included in Fig. 4a. The parameters obtained for the polymers with d_p of 106 and $90 \mu\text{m}$ were $2R_0 = 2.4 \text{ nm}$, $\sigma = 0.37$ and $2R_0 = 2.4 \text{ nm}$, $\sigma = 0.31$, respectively, and the d_{CdS} distributions are summarized in Fig. 4b. The deviation of the simulated spectra from the observed one around $480\text{--}550 \text{ nm}$ may be due to the assumption of the common line-shape function for all the transitions. Although a more sophisticated model will improve simulation, we think that the analyses are enough for the present discussion, since the shorter wavelength shift of the spectrum with decreasing d_p from 135 to $90 \mu\text{m}$ can

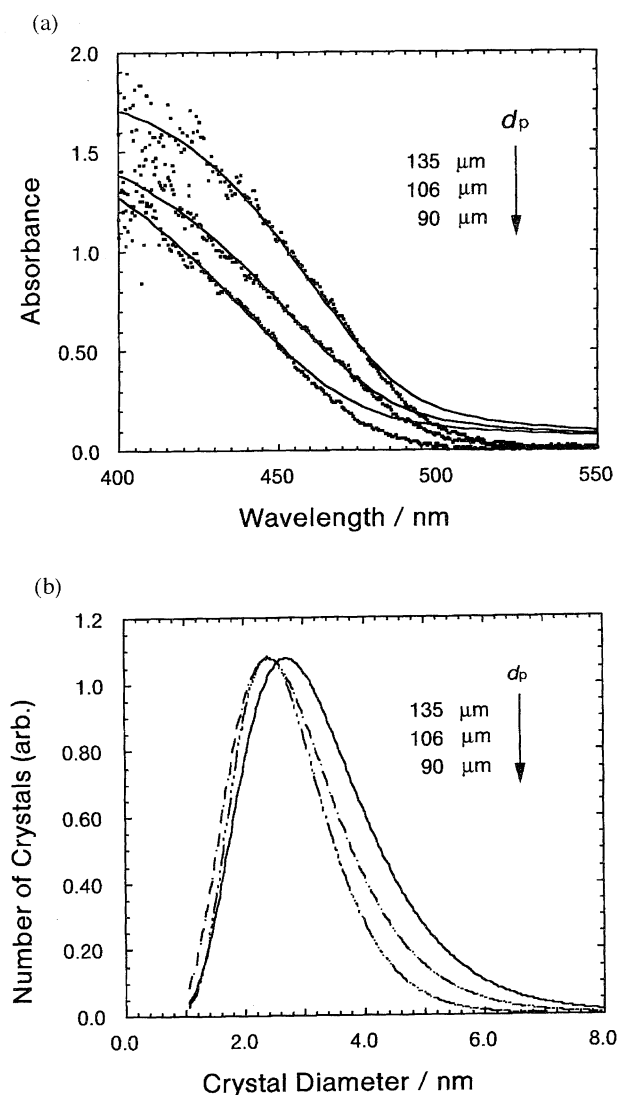


Fig. 4. Simulated absorption spectra (a) and d_{CdS} distributions (b) of sample a with various d_p .

be explained by the decreases in $2R_0$ ($2.7\text{--}2.4 \text{ nm}$) and σ ($0.37\text{--}0.31$). Furthermore, the size distribution of CdS in the polymer particle estimated by simulation is narrower for the smaller particles (Fig. 4b). Since the effective mass approximation is invalid for CdS particles smaller than $3\text{--}4 \text{ nm}$, the shift of the absorption tail to the longer wavelength can be ascribed to distributions of larger-sized CdS crystals. We concluded that the size distribution of CdS nanocrystals ($d_{\text{CdS}} > 3\text{--}4 \text{ nm}$) can be reasonably estimated by the present simulation method.

Effects of the Polymer Size and the Injection Method of Na_2S on Nanocrystalline CdS Size Distributions. The crystal size of CdS was shown to be highly dependent on both the size of the host chelate polymer particle and the injection method of an aqueous Na_2S solution (i.e., concentrated- or dilute-solution injection). The relationships between d_{CdS} and these factors are worth discussing, since this leads to the possibility of precise controls of the size and distribution of CdS nanocrystals. For sample a, since d_{CdS} and its distri-

bution are the same in both the surface and center areas of the polymer particle, nucleation of Cd^{2+} to CdS is supposed to proceed very quickly and homogeneously in the particle, which can be achieved by using micrometer-sized polymer particles as a host matrix. So the flux of S^{2-} ions in such small domains is substantially important for the formation process of CdS nanocrystals as discussed below.²²⁾

The flux of S^{2-} ions from the surrounding solution phase to the polymer surface in unit time is expressed in Eq. 4.

$$2\pi d_p D \left[1 + \frac{d_p}{2(\pi D t)^{1/2}} \right] C_0, \quad (4)$$

where D and C_0 are the diffusion coefficient and the concentration of the S^{2-} ion in the water phase, respectively.²³⁾ Nucleation in the polymer is very fast, so that the reaction between S^{2-} and Cd^{2+} proceeds via pseudo first-order kinetics. The flux of the S^{2-} ion, necessary for nucleation of Cd^{2+} ions in the polymer, can be obtained by dividing Eq. 4 by the volume of the polymer particle, $\pi d_p^3/6$. By stirring the outer solution, the transient term (the second term in the bracket in Eq. 4) can be neglected so that the flux of S^{2-} to the polymer surface is proportional to $12DC_0/d_p^2$. This indicates that, at a given C_0 , the S^{2-} flux per unit time becomes larger along with a decrease in d_p . Phenomenologically, this is what was observed for sample a. Namely, supersaturation in the smaller polymer particles proceeds more efficiently through S^{2-} diffusion, and this leads to generation of more CdS nuclei.²⁴⁾ Therefore, smaller CdS crystals are produced in the smaller polymer particles. Actually, these samples exhibited the polymer size dependence of the optical properties of the CdS nanocrystals.

For sample b, on the other hand, although the total mole number of S^{2-} in the water phase is equal to that for sample a, the concentration of S^{2-} is very low (9.2×10^{-4} M; total volume of the water phase = 60 mL) so that nucleation in the polymer phase is restricted by the low S^{2-} flux. The Cd^{2+} ions located in the surface layer of the polymer will be rapidly nucleated to CdS while the S^{2-} flux is insufficient to react with Cd^{2+} ions in the inner volume, rendering the layer-by-layer size distributions of CdS.

The effects of the host polymer particle size and the sample preparation method on d_{CdS} and its distribution are reasonably explained on the basis of the S^{2-} flux to the polymer surface and the degree of supersaturation in the polymer phase, though more detailed studies are required to elucidate the molecular mechanisms. Preparations of CdS nanocrystals in ion-exchange chelate polymer particles are very unique and we expect both d_{CdS} and its distribution will be controlled more precisely through optimization of the present preparation methods, which is in progress in our laboratory.

The authors thank Dr. Hayashi and Mr. Mizuma (Mitsui

Toatsu Chemicals, Inc.) for generously agreeing to measure the TEM images in Fig. 2.

References

- 1) M. L. Steigerwald and L. E. Brus, *Acc. Chem. Res.*, **23**, 183 (1990).
- 2) Y. Wang and N. Herron, *J. Phys. Chem.*, **95**, 525 (1992).
- 3) A. Henglein, *Chem. Rev.*, **89**, 1861 (1989).
- 4) L. Spanhel, M. Haase, H. Weller, and A. Henglein, *J. Am. Chem. Soc.*, **109**, 5649 (1987).
- 5) A. R. Kortan, R. Hull, R. L. Oplia, M. G. Bawendi, M. L. Steigerwald, P. J. Carroll, and L. E. Brus, *J. Am. Chem. Soc.*, **112**, 1327 (1990).
- 6) T. Vossmeier, L. Katsikas, M. Giersig, I. G. Popovic, K. Diesner, A. Chemseddine, A. Eychmuller, and H. Weller, *J. Phys. Chem.*, **98**, 7665 (1994).
- 7) C. B. Murray, D. B. Norris, and M. G. Bawendi, *J. Am. Chem. Soc.*, **115**, 8706 (1993).
- 8) Y. Masumoto, L. G. Zimin, K. Naoe, S. Okamoto, and T. Arai, *Mater. Sci. Eng.*, **B27**, L5 (1994).
- 9) M. Kuwata-Gonokami, N. Peyghambarian, K. Meisser, B. Fluegel, Y. Sato, K. Ema, R. Shimano, S. Mazumdar, F. Guo, T. Tokihiro, H. Ezaki, and E. Hanamura, *Nature*, **367**, 47 (1994).
- 10) V. L. Colvin and A. P. Alivisatos, *J. Chem. Phys.*, **97**, 730 (1992).
- 11) K. Misawa, H. Yao, T. Hayashi, and T. Kobayashi, *J. Chem. Phys.*, **113**, 113 (1991).
- 12) T. Teranishi, M. Harada, K. Asakura, H. Asanuma, Y. Saito, and N. Tushima, *J. Phys. Chem.*, **98**, 7967 (1994).
- 13) F. Helfferich, "Ion Exchange," McGraw-Hill, New York (1962).
- 14) Ph. Roussignol, D. Ricard, and C. Flytzanis, *Appl. Phys.*, **B51**, 437 (1990).
- 15) N. Kitamura, K. Nakatani, and H.-B. Kim, *Pure Appl. Chem.*, **67**, 79 (1995).
- 16) N. Kitamura, M. Hayashi, H.-B. Kim, and K. Nakatani, *Anal. Sci.*, **12**, 49 (1996).
- 17) J. I. Pankove, "Optical Processes in Semiconductors," Dover, New York (1971).
- 18) Y. Nosaka, *J. Phys. Chem.*, **95**, 5054 (1991).
- 19) D. W. Langer, R. N. Euwema, K. Era, and T. Koda, *Phys. Rev. B: Solid State*, **B2**, 4005 (1970).
- 20) R. A. Morgan, S.-H. Park, S. W. Koch, and N. Peyghambarian, *Semicond. Sci. Technol.*, **5**, 544 (1990).
- 21) In Ref. 14, T_2 was set 15 fs for simulation of the spectrum at low temperature. In the present study, since we measured the absorption spectra at room temperature, discrepancies between the simulated and observed spectra around the band edge were fairly large if we used the value of T_2 as 15 fs. Therefore, we used $T_2 = 10$ fs to fit more precisely the spectral band edge.
- 22) A. J. Bard and L. R. Faulkner, "Electrochemical Methods. Fundamentals and Applications," John Wiley & Sons, New York (1980).
- 23) H. Gerischer and A. Heller, *J. Phys. Chem.*, **95**, 5261 (1991).
- 24) J. J. Ramsden, *Surface Sci.*, **156**, 1027 (1985).